

# Energy consumption comparison for different quantum computing platforms

Ata Krichene

Antoine Pignalosa

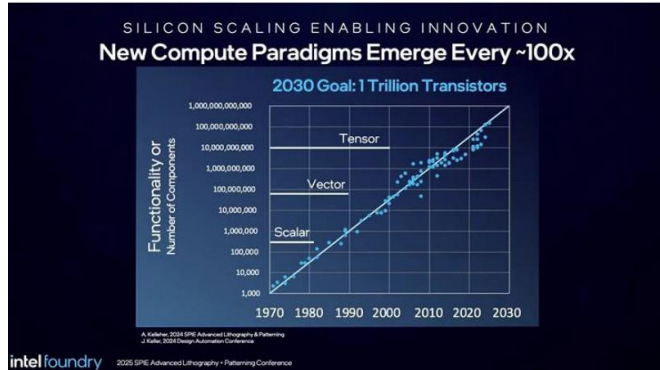
Yuchen Lu

# Content

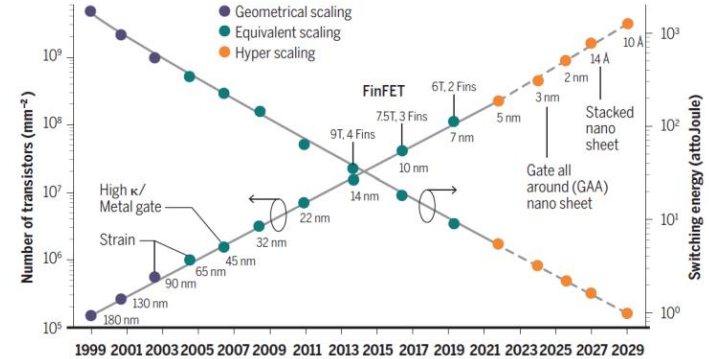
- Introduction
- Power Consumption
  - Superconducting quantum computers
  - Photonic quantum computers
  - Traped ions quantum computers
- Conclusion

# Introduction

# Moore's Law



Eric A. Karl "Evolutions in technology enabling the AI era", Proc. SPIE 13425, DTCO and Computational Patterning IV, 1342502 (23 April 2025); <https://doi.org/10.1117/12.3056887>

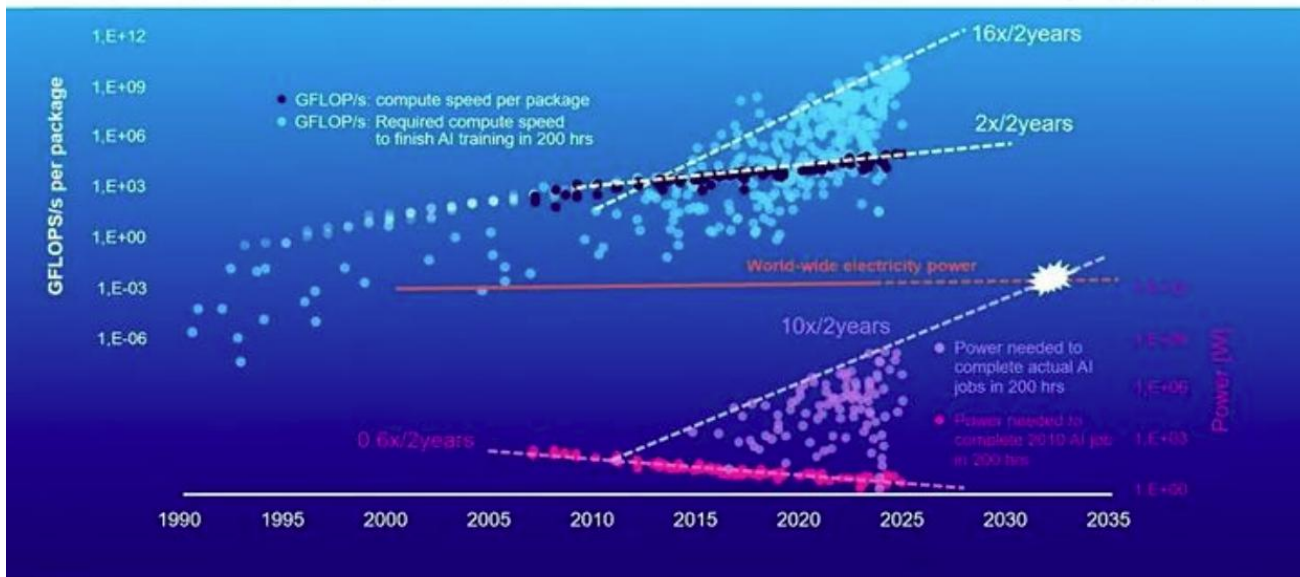


Datta, Suman, Wriddhi Chakraborty, and Marko Radosavljevic. "Toward attojoule switching energy in logic transistors." Science 378.6621 (2022): 733-740.

Miniaturization in microelectronics has enabled increased performance of integrated circuits (ICs) with reduced power consumption per device.

# AI Power Consumption

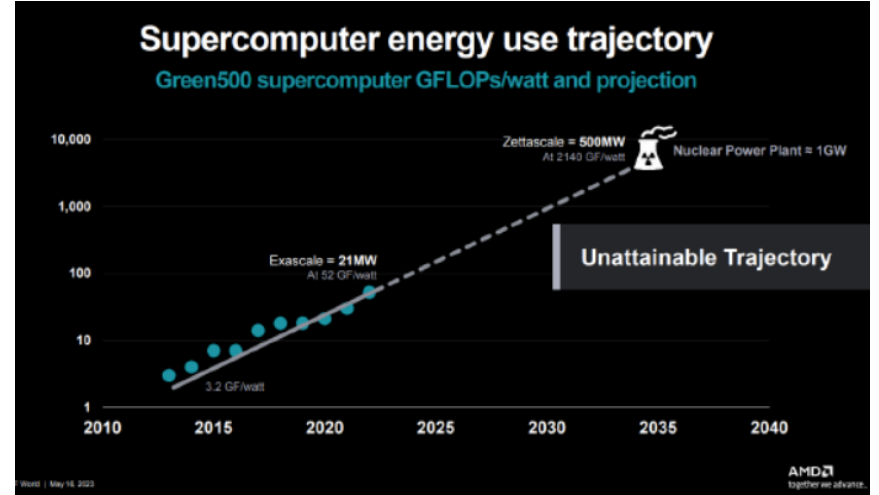
**Power needed to train a leading-edge model also outpaces Moore's law**  
 Extrapolating trend, training a leading model would use entire world-wide electricity supply by 2035



ASML

Sources: H S P Wong et al. Stanford Technology Integration Trend, accessed 2.2. 25, Epoch AI "Data on Notable AI Models" &amp; "Data on Machine Learning Hardware"

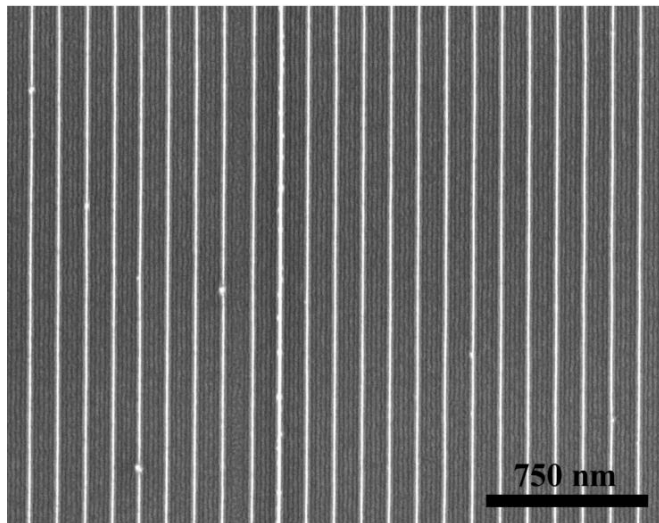
# SUPERCOMPUTING CENTERS



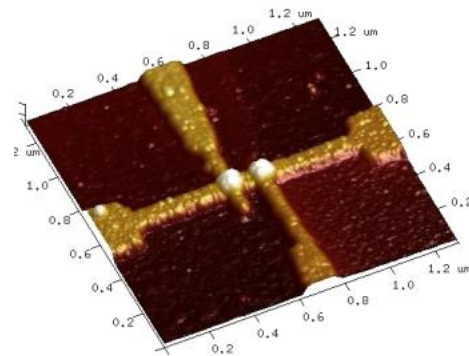
# To push the limits of current technology, research is needed

Pushing down lithography resolution

Directed self assembly of block co-polymers

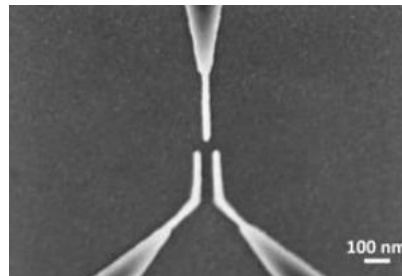


Beyond CMOS devices



Single electron devices

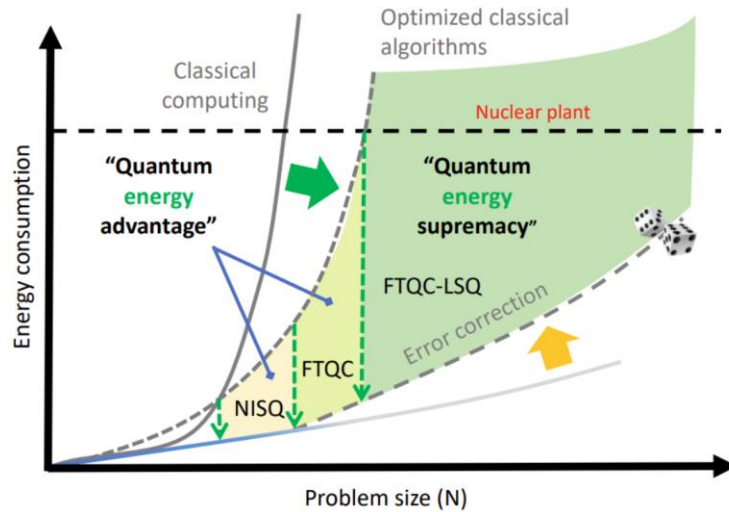
Quantum computing



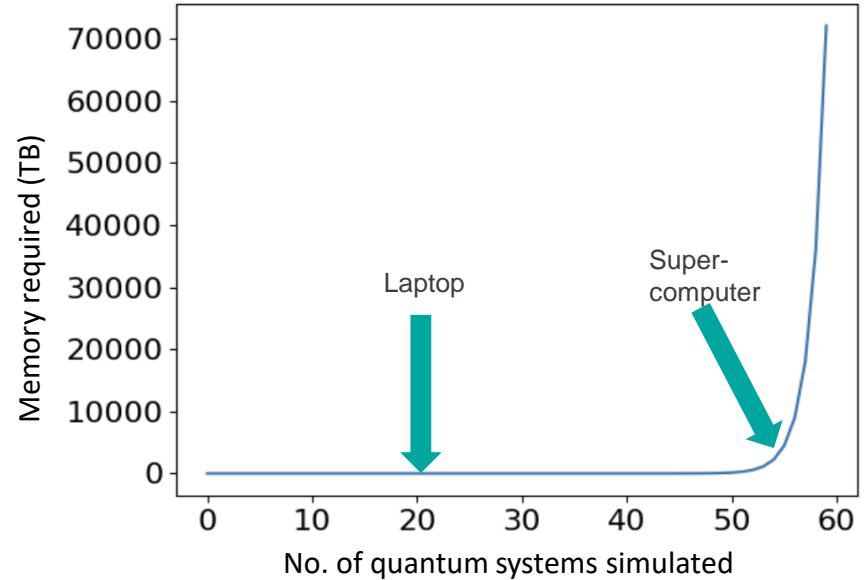
Semiconductor spin qubit

# Quantum Energy Supremacy

## Energy consumption



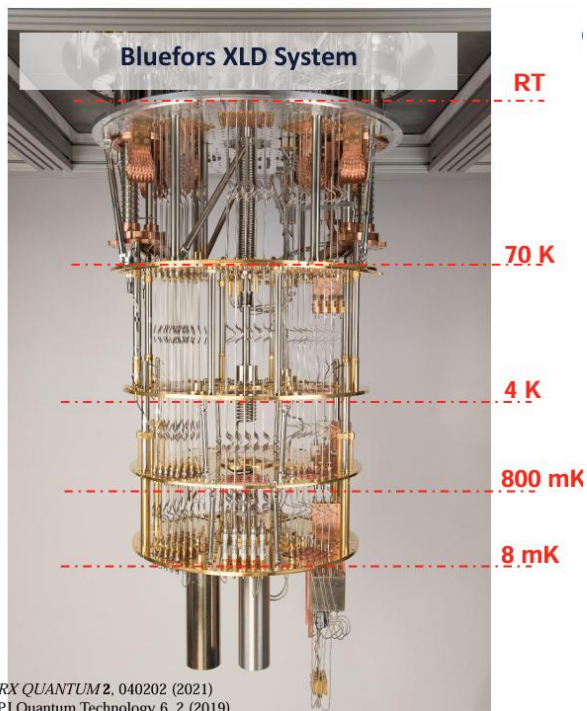
## Memory needed to simulate quantum systems



# Three quantum computing platforms

# Superconducting platform

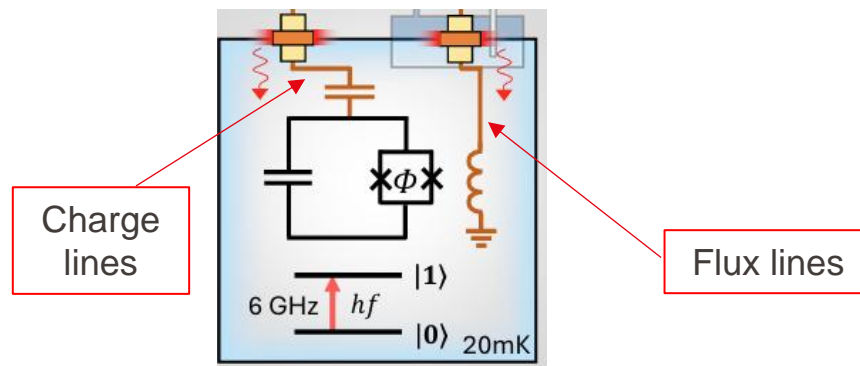
# Superconducting Qubits in a Dilution Refrigerator



Superconducting circuits are operated at 20 mK where the quantum system can be initialized in its ground state and avoid spurious thermal excitations.

Dilution refrigerators provide critical cooling and isolation

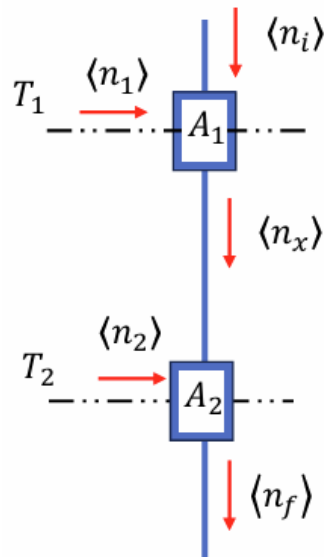
- Control lines for each qubit (Coaxial cables):
- Microwave lines for driving state transitions.
  - DC current-carrying lines for parametric control



- In a coaxial cable connecting room temperature electronics to base temperature circuits, thermal photons number is:
  - $\langle n_{th} \rangle \approx 10^3$
- For quantum applications:
  - $\langle n_{th} \rangle \approx 10^{-3}$
- In order to suppress thermal noise, attenuators must be introduced along the microwave lines.

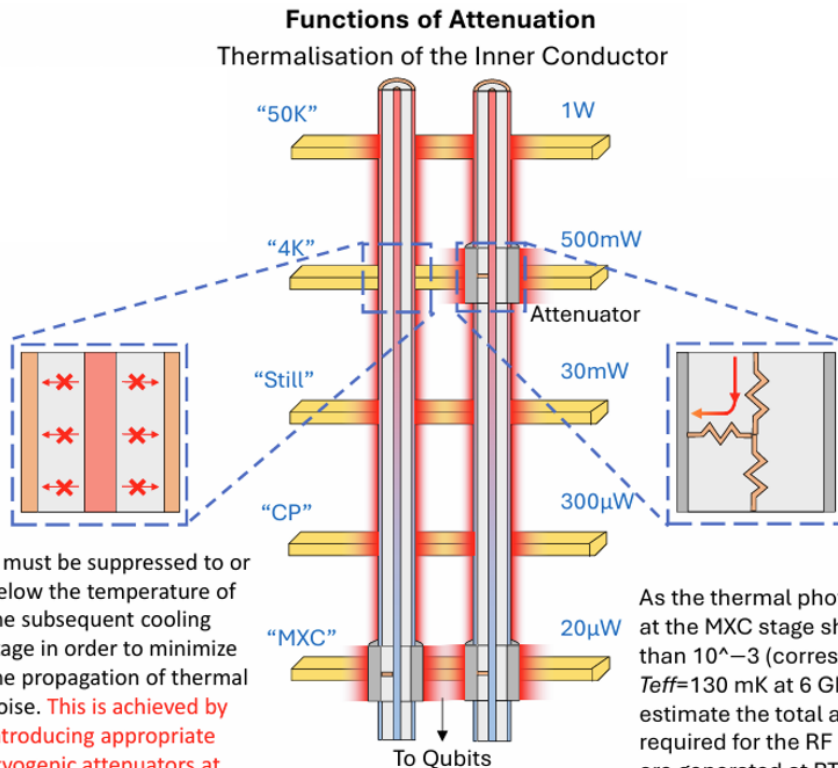
## Noise-photon spectral density

$$n_{\text{BE}}(T, \omega) = \frac{1}{e^{\frac{\hbar\omega}{k_{\text{B}}T}} - 1}$$



$$\langle n_f \rangle = \frac{\langle n_i \rangle}{A_1 A_2} + \left(1 - \frac{1}{A_1}\right) \frac{\langle n_1 \rangle}{A_2} + \left(1 - \frac{1}{A_2}\right) \langle n_2 \rangle,$$

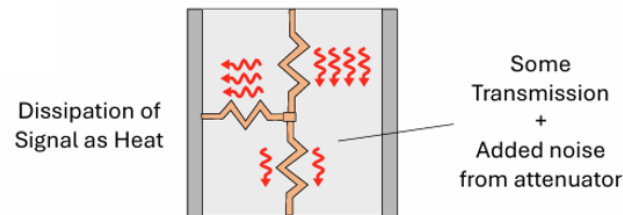
# Attenuators – Microwave Lines



It must be suppressed to or below the temperature of the subsequent cooling stage in order to minimize the propagation of thermal noise. This is achieved by introducing appropriate cryogenic attenuators at each temperature stage.

As the thermal photon occupation at the MXC stage should be smaller than  $10^{-3}$  (corresponding to  $T_{eff}=130$  mK at 6 GHz), we can estimate the total attenuation required for the RF signals that are generated at RT from:

Suppression of Blackbody Noise  
(+ Attenuation of Signal Power)



### Delicate Balance

Attenuation on hotter stages for alleviating heat

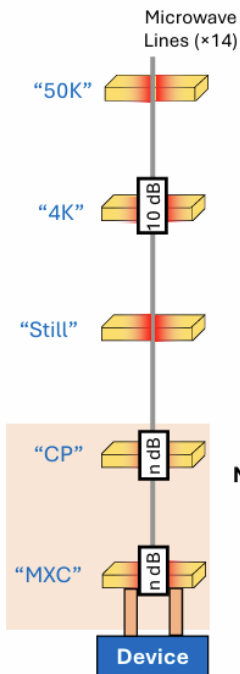
Attenuation on colder stages for low noise “temperature”

How much attenuation do we need?

$$\frac{n_{th}(300K, 6GHz)}{n_{th}(10mK, 6GHz)} \approx 60dB$$

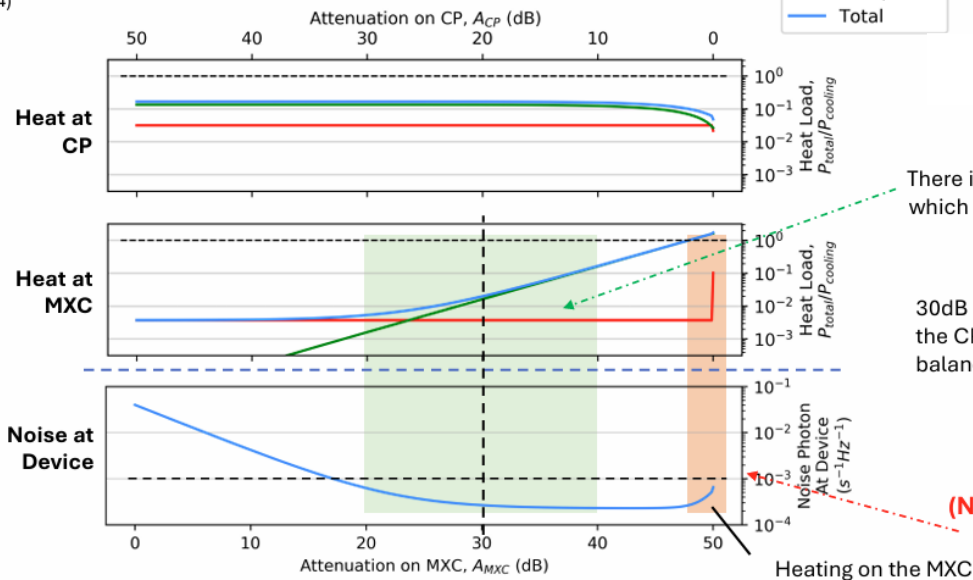
# Microwave Line Attenuators

## Splitting 50dB Attenuation on the Lower Stages



### The noise photon occupation number

$$n(T, \omega) = n_{in} 10^{-\frac{A}{10}} + (1 - 10^{-\frac{A}{10}}) n_{BE}(T, \omega)$$



A. T. Di Lonardo, Optimising Cryogenic Wiring for Superconducting Qubit Processors in a Dilution Refrigerator, University of Technology Sydney

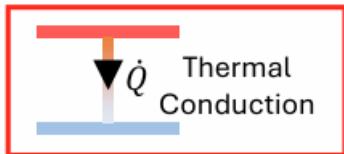
There is a large set of solutions which meet the heat and noise constraints

30dB on the MXC and 20dB on the CP, which strikes a good balance of heat and noise

(Noise Target:  $10^{-3}$  noise photons)

Splitting 50dB between the CP stage and MXC stage

# Heat Flux and cryogenic Power consumption



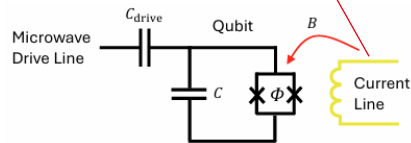
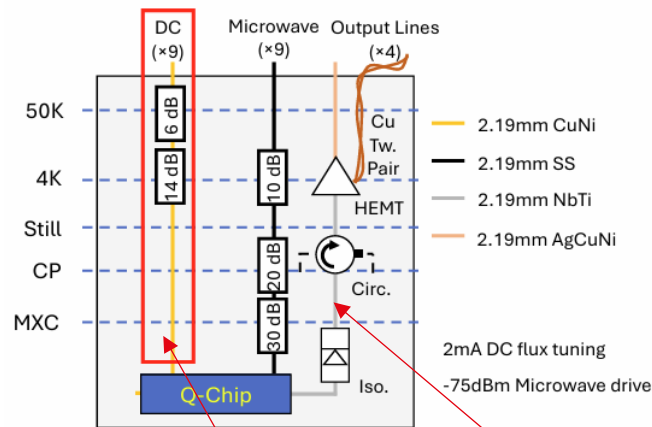
At each stage:

$$\dot{Q}_i = A_i P_{i-1}$$

- Using an optimal Carnot cycle:

$$\bullet \frac{P_{cryo,i}}{\dot{Q}_i} = \frac{T_{i-1} - T_i}{T_i}$$

$$\bullet P_{cryo} = \sum_i P_{cryo,i} = \sum_i \left( \frac{T_{i-1}}{T_i} - 1 \right) A_i P_{i-1}$$

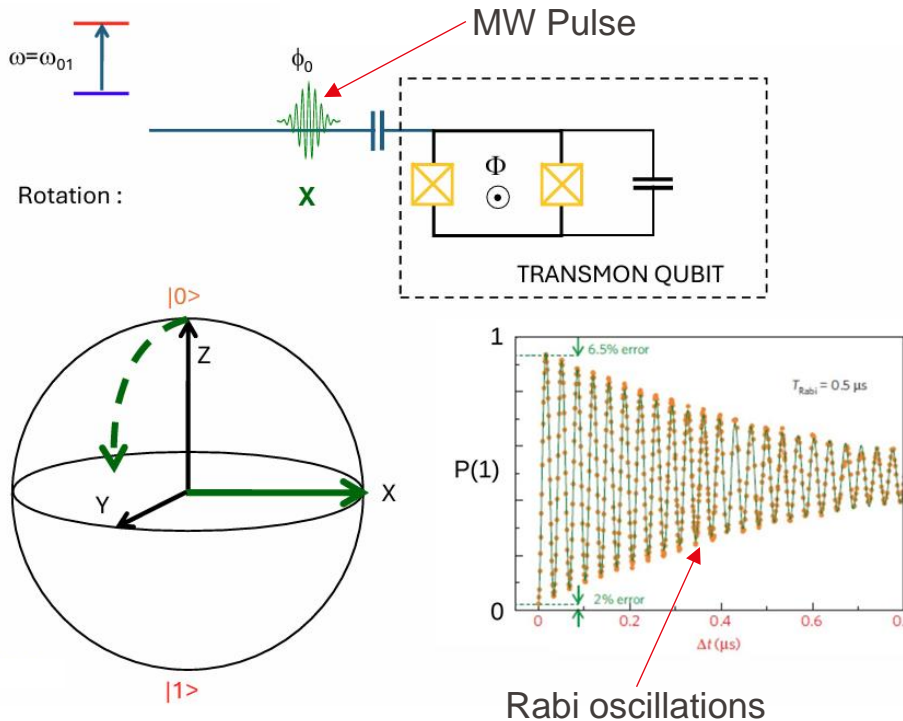


Readout lines  
~No Power consumption

Typically, weakly coupled to qubits  
→ Need less attenuation (~20dB)

6dB on 50K and 14dB on 4K is ideal

# Power consumption at chip level (X-gate)



$$H_F = \underbrace{-\frac{\hbar\omega_{01}}{2}\sigma_z}_{H_{qb}} + \underbrace{gE\cos(\omega t)(\sigma_+ + \sigma_-)}_{H_{drive}}$$

In the Rotating frame+RWA:

$$H_F = \frac{\hbar\Delta}{2}\sigma_z + \frac{\hbar\Omega}{2}(\sigma_+ + \sigma_-)$$

Detuning

Rabi frequency

$$\Omega \propto \frac{gE}{\hbar}$$

X-gate is performed by setting:

- $\Delta = 0$
- $\tau_\pi = \frac{\pi}{\Omega} = \frac{T_{Rabi}}{2}$

# Decoherence and Power consumption

Assuming a weak coupling to a Thermal bath:

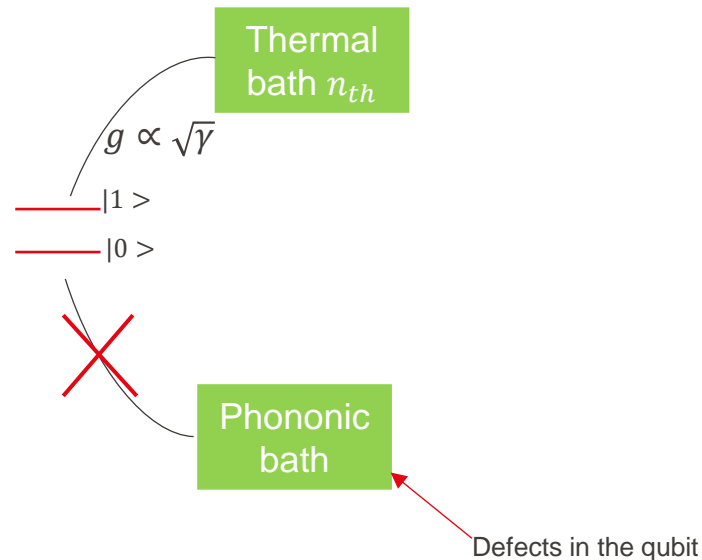
- Spontaneous emission ( $\gamma$ )
- Stimulated emission ( $\gamma n_{th}$ )
- Absorption ( $\gamma n_{th}$ )

Power consumption:

$$P = \hbar\omega (a^\dagger a)^2 \propto \hbar\omega E^2 \stackrel{\Omega \propto gE}{=} \Omega^2 \frac{\hbar\omega}{\gamma}$$

For a X-gate:  $P_\pi = \frac{\pi^2 \hbar\omega}{4 \gamma \tau_\pi^2}$

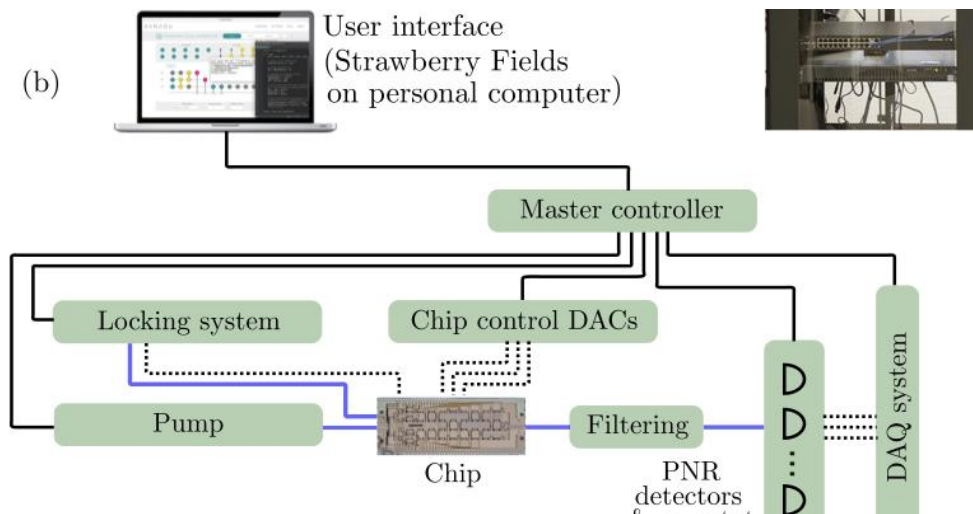
Fidelity:  $F = 1 - P_{error} = 1 - \underbrace{\gamma(n_{th} + 1)}_{\text{Emission rates}} \tau_\pi$



$$P_\pi = \frac{\pi^2 \hbar\omega \gamma (n_{th} + 1)^2}{4 (1 - F)^2}$$

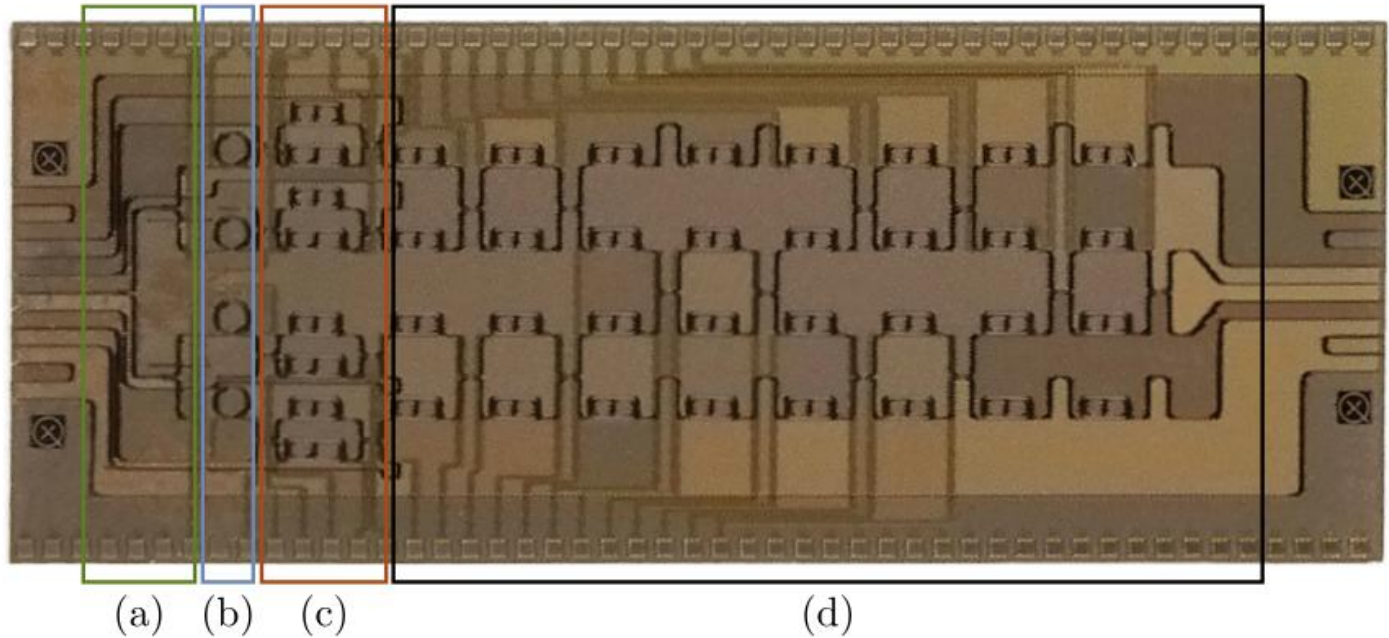
# Photonic platforms

# The overview of the platform



## Quantum circuits with many photons on a programmable nanophotonic chip

Xanadu's  
design, Toronto C  
anada.  
The  
chip is  
approximately  
10 mm×4 mm  
in size.



- a) Input power distribution tree
- b) Squeezer array
- c) AMZI filter array
- d) Programmable unitary transformation.

# Power consumption of the different components

Laser sources: Lasers as Pump Sources for Single-photon or Photon Pair Emitters

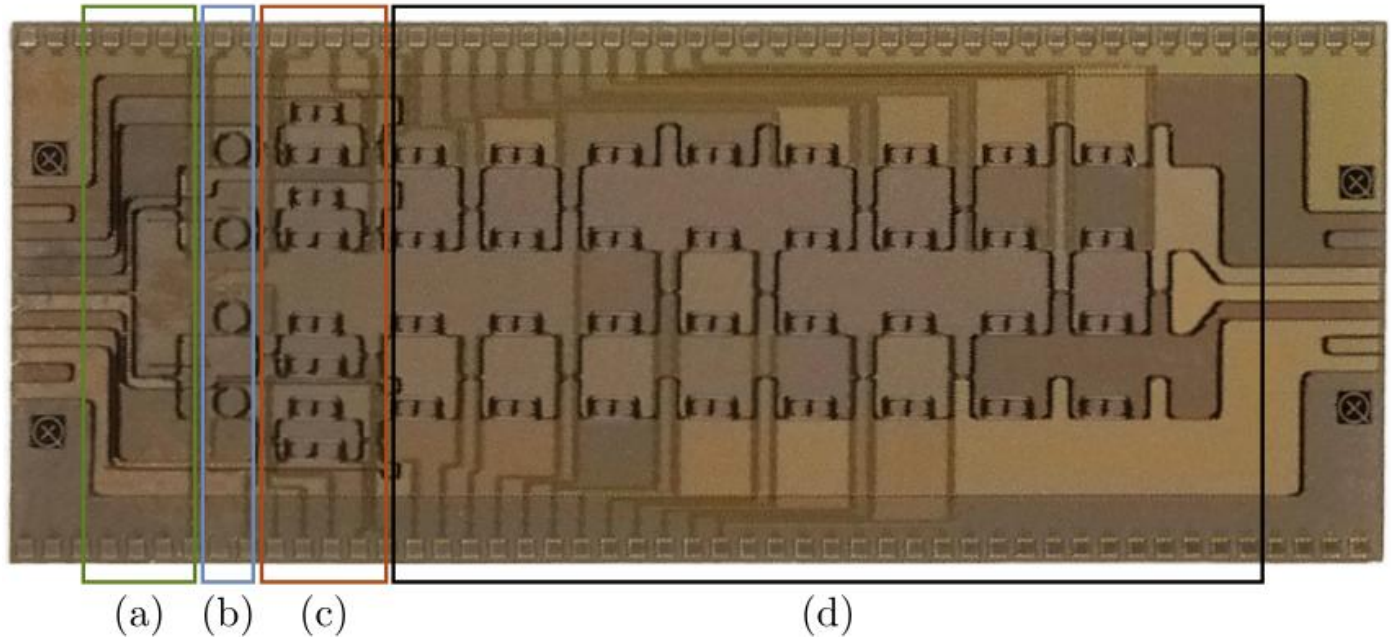
Need for short and intense pulses of light: pulsed laser



"Local" data: **DQML** at EPFL.  $P_{laser} = 1023W$   
→ 0.6% conversion between electrical power and optical power.

## Quantum circuits with many photons on a programmable nanophotonic chip

Xanadu's  
design, Toronto C  
anada.



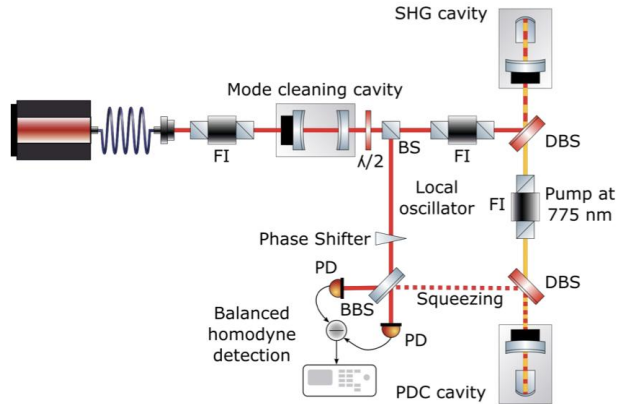
- a) Input power distribution tree
- b) **Squeezer array**
- c) AMZI filter array
- d) Programmable unitary transformation.

# Squeezers

## PHOTONICS Research

13 dB Squeezed Vacuum States at 1550 nm from 12 mW external pump power at 775 nm

AXEL SCHÖNBECK<sup>1</sup>, FABIAN THIES<sup>2</sup>, AND ROMAN SCHNABEL<sup>1</sup>



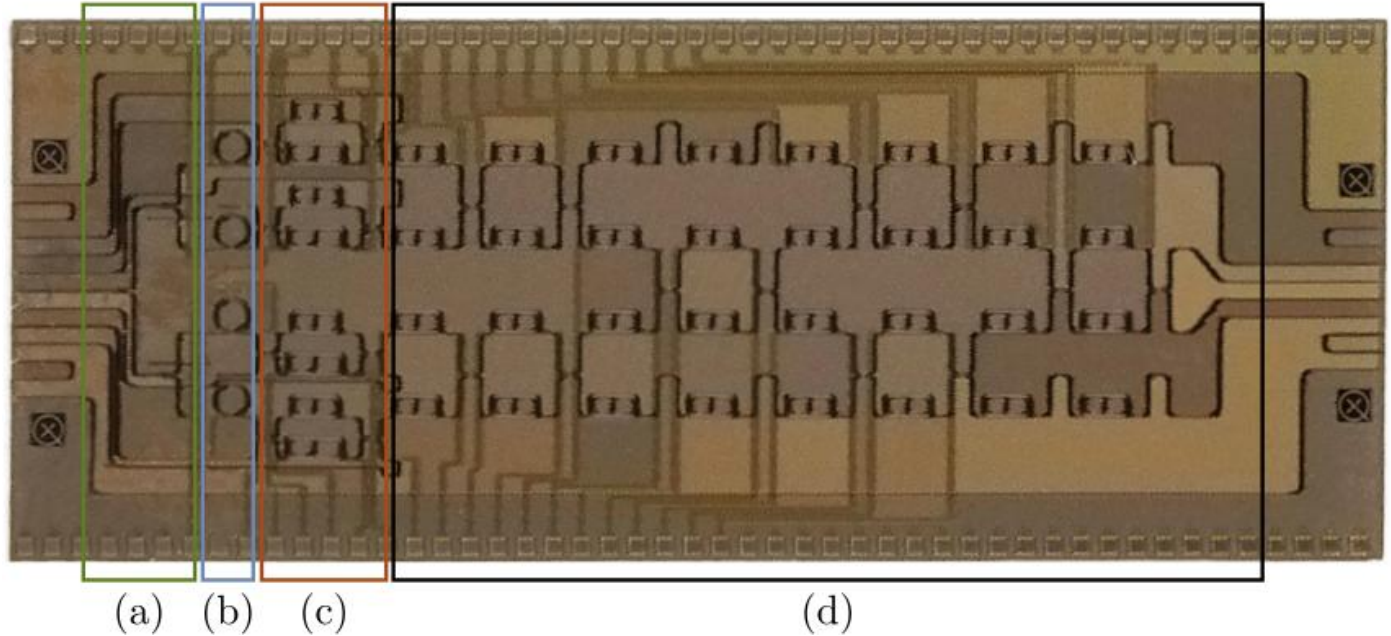
Topologically protecting squeezed light on a photonic chip

University of Shanghai demonstrates also that it is possible to achieve squeezed states of light on nanophotonic chip

$$\frac{P_{\text{cav}}}{P_{\text{pump}}} = \frac{(1 - R_1)}{(1 - \sqrt{R_1 R_2} V)^2}$$

## Quantum circuits with many photons on a programmable nanophotonic chip

Xanadu's  
design, Toronto C  
anada.



- a) Input power distribution tree
- b) Squeezer array
- c) AMZI filter array
- d) **Programmable unitary transformation.**

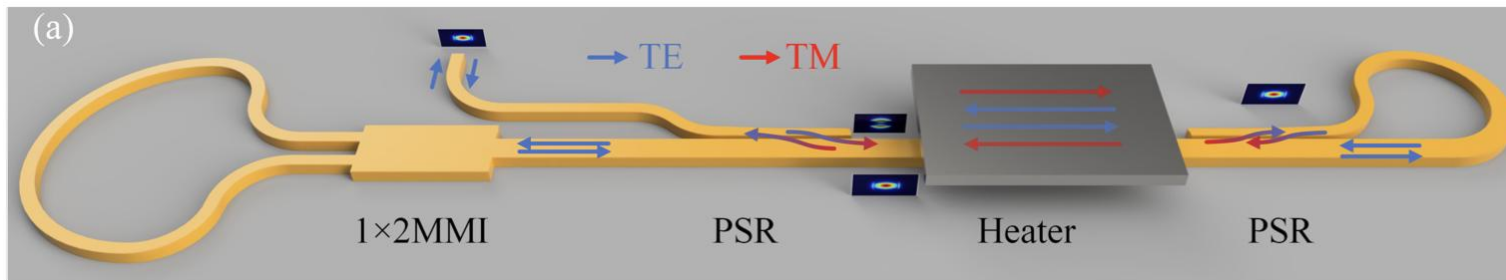
## High-efficiency Thermo-optical Phase Shifter using Wave-vector and Polarization Multiplexing

Zhen Wang, Qihang Shang, Yong Zhang, Yikai Su\*

*State Key Lab of Advanced Optical Communication Systems and Networks, Department of Electronic Engineering, Shanghai Jiao Tong University, Shanghai 200240, China*

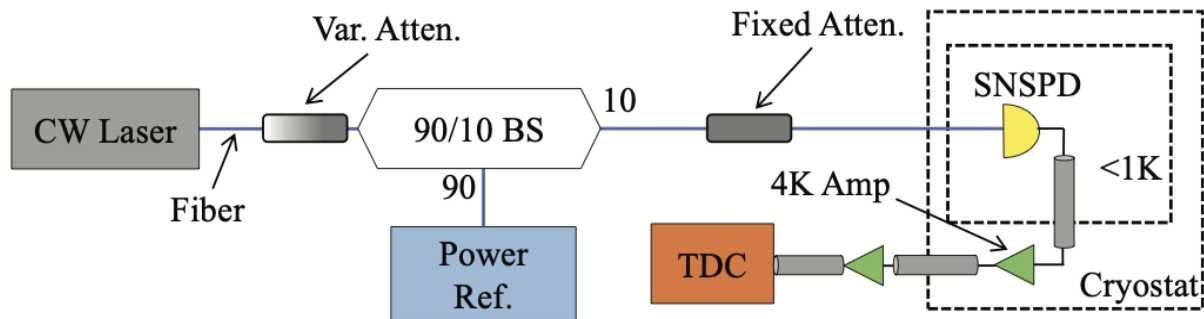
*yikaisu@sjtu.edu.cn*

**Abstract:** We demonstrate a four-pass thermo-optic phase shifter using wave-vector and polarization multiplexing. The experiment shows that the structure reduces the power consumption of a phase shifter by 3.2 times with a 3.1-dB insertion loss. © 2021 The Author(s)



# Single photon detector

*Scalable Cryogenic Read-out Circuit for a Superconducting Nanowire Single-Photon Detector System, Duke University*



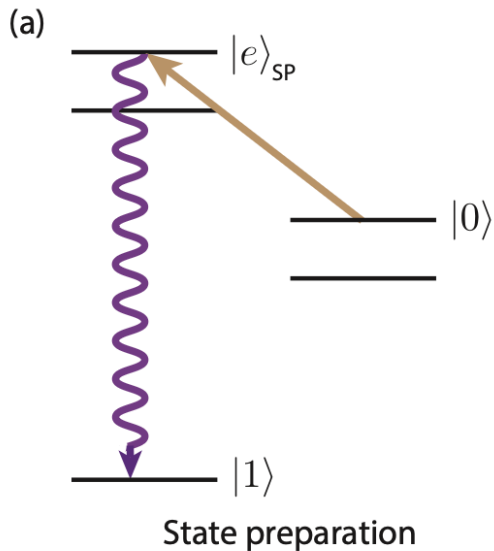
This design demonstrates a **35 ps timing resolution** and a **maximum count rate of over 20 million counts per second** while **maintaining < 3 mW power consumption per channel**, making it suitable for a multichannel read-out.

# Single photon detector at room temperature ?

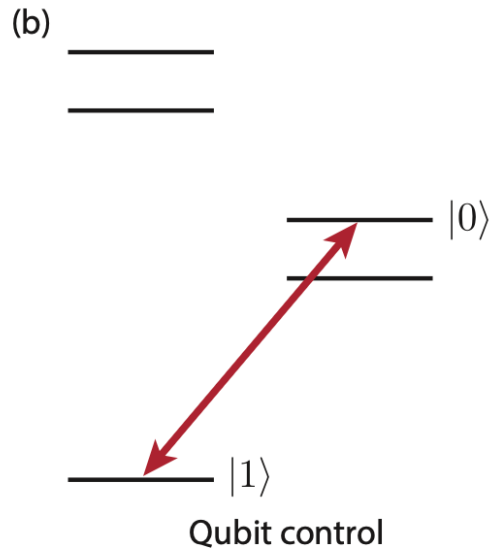
- **Single-Photon Avalanche Diodes (SPADs):**  
Based on silicon or InGaAs diodes operated in Geiger mode.
  - **Si SPADs:** Efficient for visible and near-infrared (~400–1000 nm). **InGaAs SPADs** can reach telecom wavelength but with higher noise.
  - **Advantages:** Compact, low power, commercially available
  - **Inconvenient:** Dark counts (false counts due to thermal excitations) increase at room temperature. Temporal jitter is higher than in superconducting detectors (~tens to hundreds of ps versus tens of ps) .
- **Photomultiplier Tubes (PMTs):**  
Vacuum tubes that multiply a single photoelectron signal.
  - Usable in UV to near-IR.
  - **Advantages:** High gain, fast response.
  - **Inconvenient:** Bulky, need magnetic shielding. Moderate quantum efficiency 20-30% (probability that an incoming photon is successfully detected). Sensitive to noise at room temperatures

# Trapped-Ion platform

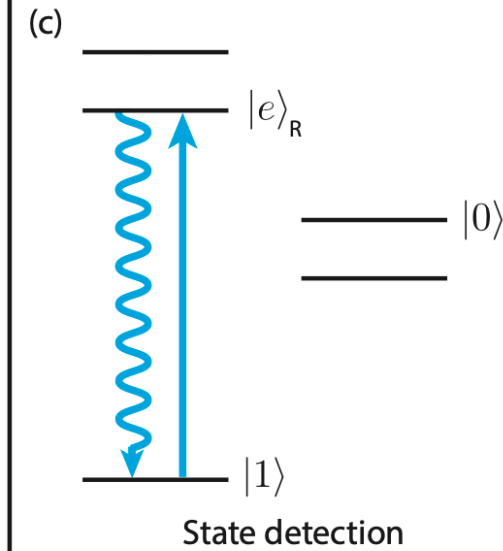
# Overview of trapped-ion quantum computing



The ion is optically pumped to the  $|1\rangle$  state by coupling the long-lived  $|0\rangle$  state to an auxiliary state  $|e\rangle_{SP}$  that rapidly decays.



Qubit control is achieved by directly coupling the  $|0\rangle$  and  $|1\rangle$  states using a narrow electric quadrupole transition.



Readout is achieved by shining light resonant on the broad transition  $|1\rangle \rightarrow |e\rangle_R$ , and collecting the resulting scattered fluorescence photons.

No transition  $|0\rangle \rightarrow |e\rangle_R$  and  $|0\rangle$  appears dark.



## Definition

An ion trap is a device whose purpose is to keep ions confined within a narrow region of space.

- A trapped ion will behave like a **simple harmonic oscillator**.
- **Linear traps:** a strong Paul trap in  $x$  and  $y$  direction with a relatively weaker pair of electrodes in  $z$  direction.

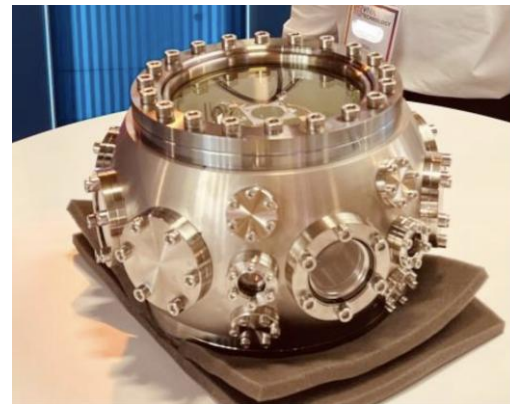
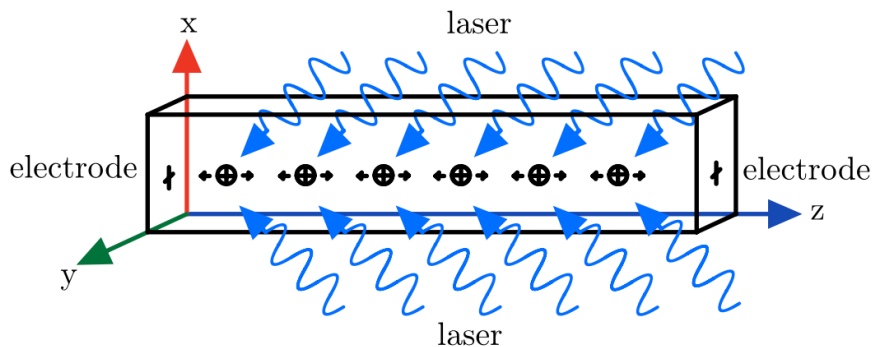


Figure: A vacuum chamber from *Pasqal*, which contains a magneto-optical trap and a laser cooling system

- **Linear Radio-Frequency Paul Trap (RF Paul trap):**

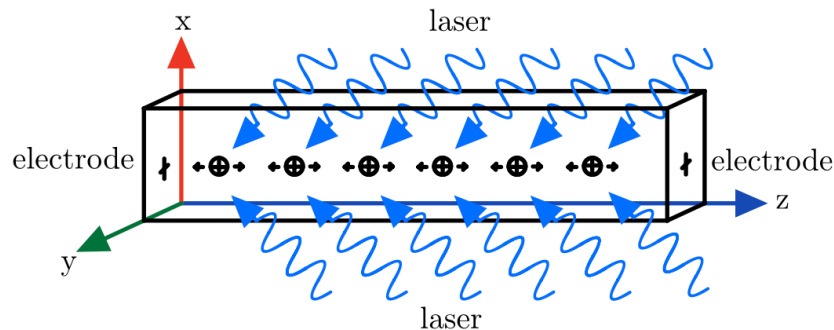
- $\Omega_{\text{RF}}$ : Angular frequency of the RF source;
- $q$ : Electric charge on the trapped particle;
- $m$ : Mass of the ion;
- $r_0$ : Characteristic trap dimension;
- $U_{\text{DC}}$ : Static voltage applied to provide axial confinement
- $V_0$ : Amplitude of RF voltage.

The ion's motion in  $x$  and  $y$  direction obeys the **Mathieu equation**:

$$\frac{d^2x}{d\xi^2} + [a_x - 2q_x \cos(2\xi)]x = 0$$

where

$$\xi = \frac{\Omega_{\text{RF}}}{2}t, \quad q_x = \frac{2qV_0}{m\Omega^2 r_0^2}, \quad a_x = \frac{4qU_{\text{DC}}}{m\Omega^2 r_0^2}.$$



- **The total Hamiltonian:**

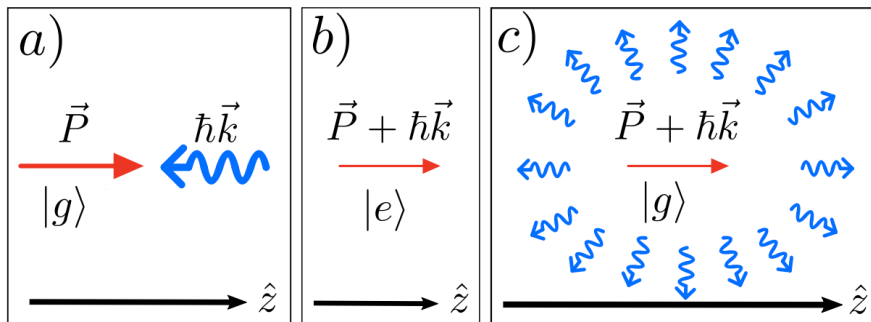
$$H = H_a + \frac{P_z^2}{2m} + \frac{1}{2}mw_z^2z^2$$

- **Power consumption :**

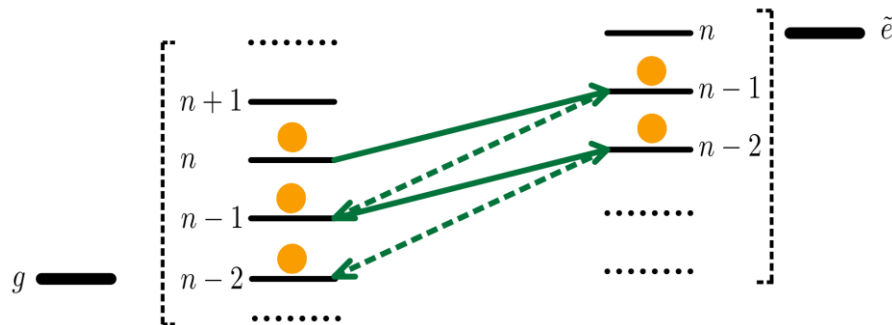
- RF:  $P \propto V_0^2 \cdot \Omega_{\text{RF}} \cdot C_{\text{RF}}$
- DC: negligible.

We have two regimes in the cooling procedure:

- A **classical** regime: the ion can be considered a classical spring, and quantum phenomena can be neglected.
- A **quantum** regime: the energy is comparable to  $\hbar\omega_z$ , and quantum effects becomes significant.



- For classical regime, we use doppler cooling, where an ion absorbs a red-shifted laser coming towards it and emits it in a random direction.



- For quantum regime, we use sideband cooling. We apply the laser pulse for a time  $\Delta t$ , which drive the state from  $|g, n\rangle$  to  $|e, n-1\rangle$ . Then the ion spontaneously decays from  $|e, n-1\rangle$  to  $|g, n-1\rangle$ .

- We have three different kinds of transitions:
  - Carrier:  $\{|g, n\rangle \leftrightarrow |e, n\rangle\}$
  - Blue sideband:  $\{|g, n\rangle \leftrightarrow |e, n + 1\rangle\}$
  - Red sideband:  $\{|g, n\rangle \leftrightarrow |e, n - 1\rangle\}$

- The time-evolution operator:

$$U = \begin{pmatrix} \cos\left(\frac{\beta}{2}\right) & -ie^{-i\phi} \sin\left(\frac{\beta}{2}\right) \\ -ie^{-i\phi} \sin\left(\frac{\beta}{2}\right) & \cos\left(\frac{\beta}{2}\right) \end{pmatrix}$$

with different basis for different transitions.

$\beta = \Omega t$  for carrier transitions;

$\beta = \eta\Omega t$  for sideband transitions.

- The Hamiltonians for three transitions:

Carrier:

$$H_I^{(c)} \approx \frac{1}{2} \hbar \Omega (\sigma_+ e^{i\phi} + \sigma_- e^{-i\phi})$$

Blue sideband:

$$H_I^{(\text{bsb})} \approx \frac{1}{2} \hbar \eta \Omega (a^\dagger \sigma_+ e^{i\phi} + a \sigma_- e^{-i\phi})$$

Red sideband:

$$H_I^{(\text{rsb})} \approx \frac{1}{2} \hbar \eta \Omega (a \sigma_+ e^{i\phi} + a^\dagger \sigma_- e^{-i\phi})$$

- **Power consumption:**

$$E \approx P_{\text{laser on}} \times t_{\text{pulse}}$$

# Manipulation of multiple ions

- For linear traps at usual working temperatures for QC experiments, ions tend to form coherent chain-like structures called **Coulomb crystals**.
- The ions in this crystal can still be considered as individual atomic qubits, but from a motional point of view they have to be regarded as a **lattice**.
- The chain of  $N$  ions must be described as  $N$  individual atomic qubits and one global vibrational qubit

$$\{|a_1, \nu_1\rangle, \dots, |a_n, \nu_n\rangle\} \rightarrow \{|a_1, \dots, a_n, \nu\rangle\}$$

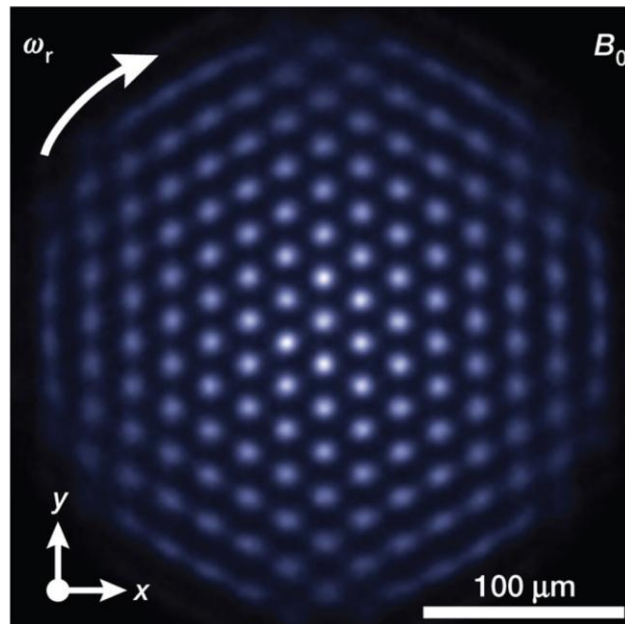


Figure: An image of an ion Coulomb crystal consisting of a single plane of  $\text{Be}^+$  ions in a Penning trap.

- Recall the time-evolution operator:

$$U = \begin{pmatrix} \cos\left(\frac{\beta}{2}\right) & -ie^{-i\phi} \sin\left(\frac{\beta}{2}\right) \\ -ie^{-\phi} \sin\left(\frac{\beta}{2}\right) & \cos\left(\frac{\beta}{2}\right) \end{pmatrix}$$

with different basis for different transitions.  $\beta = \Omega t$  for carrier transitions;  $\beta = \eta\Omega t$  for sideband transitions.

- Swap gate between atomic and vibrational states:**

Realized by the red sideband transition, with a laser pulse of  $\beta = \pi$  and  $\tilde{\phi} = \frac{3\pi}{2}$ .

$$\text{SWAP}_{av} := \begin{pmatrix} |g, 0\rangle & |g, 1\rangle & |e, 0\rangle & |e, 1\rangle \\ 1 & 0 & 0 & 0 \\ 0 & 0 & 1 & 0 \\ 0 & -1 & 0 & 0 \\ 0 & 0 & 0 & 1 \end{pmatrix} \begin{matrix} |g, 0\rangle \\ |g, 1\rangle \\ |e, 0\rangle \\ |e, 1\rangle \end{matrix}$$

■

- Hadamard gate:**

Realized by the carrier transition, with a laser pulse of  $\beta = \frac{\pi}{2}$  and  $\phi = -\frac{\pi}{2}$  followed by another laser pulse of  $\beta = \pi$  and  $\phi = \pi$ , i.e.,

$$H = U^{(c)}(\beta = \pi, \phi = \pi) \cdot U^{(c)}\left(\beta = \frac{\pi}{2}, \phi = -\frac{\pi}{2}\right)$$

- CZ gate between atomic and vibrational states ( $CZ_{av}$ ):**

Realized by the blue sideband transition, with a laser pulse of  $\beta = 2\pi$ .

$$CZ_{av} := \begin{pmatrix} |g, 0\rangle & |g, 1\rangle & |e, 0\rangle & |e, 1\rangle \\ 1 & 0 & 0 & 0 \\ 0 & 1 & 0 & 0 \\ 0 & 0 & 1 & 0 \\ 0 & 0 & 0 & -1 \end{pmatrix} \begin{matrix} |g, 0\rangle \\ |g, 1\rangle \\ |e, 0\rangle \\ |e, 1\rangle \end{matrix}$$

- The total power required for a single-qubit Raman excitation with Rabi frequency  $\Omega_R$ , while achieving a certain error probability  $\epsilon_R$

$$P_{\text{Raman,1Q}} = \frac{4\pi}{3} \hbar c w_0^2 \frac{k_{3/2}^3}{\epsilon_R} \Omega_R = \frac{2\pi^2}{3} \hbar c w_0^2 \frac{k_{3/2}^3}{\epsilon_R} t_{\text{gate}}^{-1}.$$

- For two-qubit Raman gates, the required power is

$$P_{\text{Raman,2Q}} = \frac{16\pi^2}{3} c w_0^2 \frac{k_{3/2}^3}{\epsilon_R} m \omega_T t_{\text{gate}}^{-1}$$

- The total power required for a single-qubit optical transition with Rabi frequency  $\Omega_Q$  on a quadrupole transition with wavevector magnitude  $k_D$  to a  $D$  state with decay rate  $\gamma_D$ :

$$P_{\text{Opt,1Q}} = \frac{1}{10} \hbar c w_0^2 \frac{k_D^3}{\gamma_D} \Omega_Q^2 = \frac{\pi^2}{40} \hbar c w_0^2 \frac{k_D^3}{\gamma_D} t_{\text{gate}}^{-2}.$$

- For two-qubit optical gates, the required power is

$$P_{\text{Opt,2Q}} = \frac{\pi^2}{10} c w_0^2 \frac{k_D^3}{\gamma_D} m \omega_T t_{\text{gate}}^{-2}.$$

Ion	Single-qubit gate ( $\leq 10^{-4}$ error)		Two-qubit gate ( $\leq 10^{-3}$ error)	
	$t_{C-O,1Q}$ (ns)	$P(t_{C-O,1Q})$ (mW)	$t_{C-O,2Q}$ ( $\mu$ s)	$P(t_{C-O,2Q})$ (mW)
$^{43}\text{Ca}^+$	680	5.0	12	3.9
$^{87}\text{Sr}^+$	290	10	3.9	22
$^{137}\text{Ba}^+$	2300	0.97	170	0.73
$^{171}\text{Yb}^+$	14	420	0.11	2000

# Power consumption of quantum gates

$$P_{\text{Raman},1\text{Q}} = \frac{4\pi}{3} \hbar c w_0^2 \frac{k_{3/2}^3}{\epsilon_R} \Omega_R = \frac{2\pi^2}{3} \hbar c w_0^2 \frac{k_{3/2}^3}{\epsilon_R} t_{\text{gate}}^{-1}.$$

$$P_{\text{Opt},1\text{Q}} = \frac{1}{10} \hbar c w_0^2 \frac{k_D^3}{\gamma_D} \Omega_Q^2 = \frac{\pi^2}{40} \hbar c w_0^2 \frac{k_D^3}{\gamma_D} t_{\text{gate}}^{-2}.$$

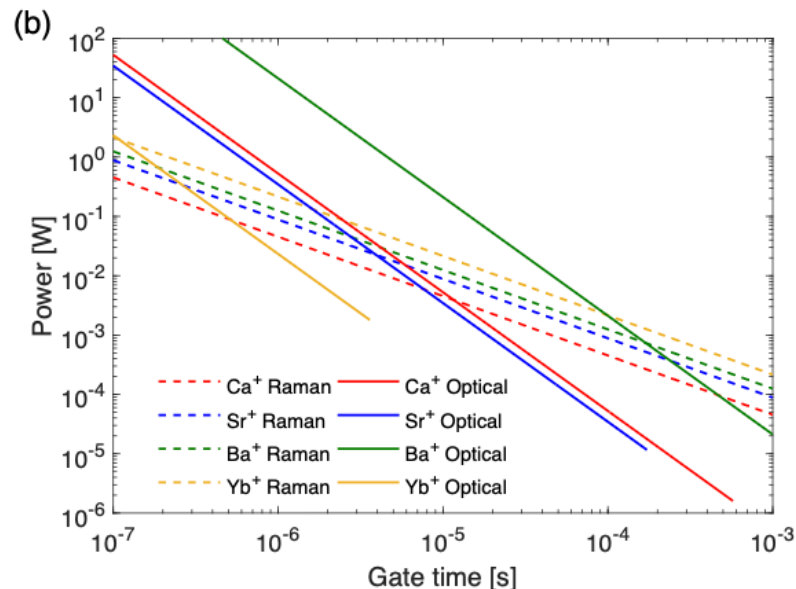
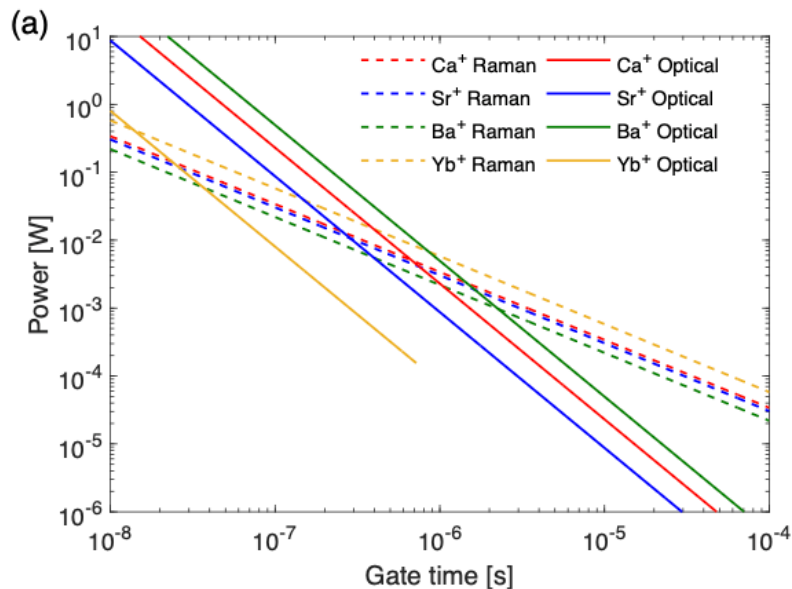
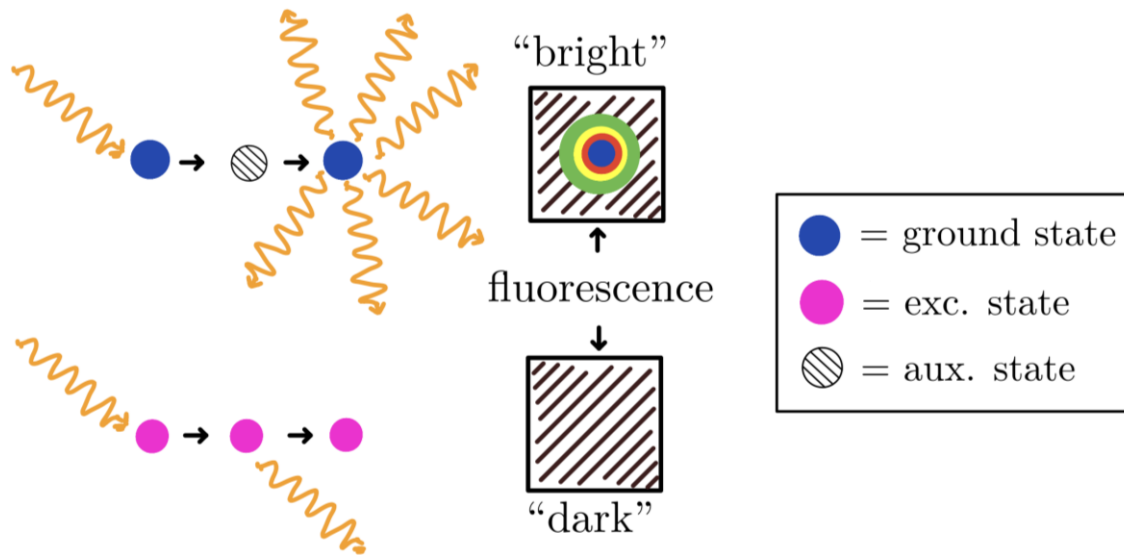


Figure: Optical power required to drive optical and Raman gates as a function of gate time for several ion species of interest.



- States involved:

- Ground state:  $|1\rangle$  (bright state)
- Auxiliary excited state:  $|e'\rangle$
- Excited state:  $|0\rangle$  (dark state)

- High-fidelity readout:

- For an optical qubit stored in the  $(4S_{1/2}, 3D_{5/2})$  levels of  $\text{Ca}^+$ , the readout fidelity  $\geq 99.991(1)\%$

# Power consumption of trapped-ion quantum computing

- Power consumption of state preparation:

$$P_1 = P_{\text{trap}} + P_{\text{laser pulse}} + P_{\text{cooling}} + P_{\text{vacuum pump}} + P_{\text{control electronics}}$$

- $P_{\text{trap}} \propto V_0^2 \cdot \Omega_{\text{RF}} \cdot C_{\text{RF}} \sim 50 \text{ to } 100 \text{ W}$
- $P_{\text{laser pulse}} \sim 1 \text{ to } 5 \text{ W}$
- $P_{\text{vacuum pump}} \sim 250 \text{ W}$

- Power consumption of state control:

$$P_2 = P_{\text{trap}} + P_{\text{laser pulse}} + P_{\text{vacuum pump}} + P_{\text{control electronics}}$$

- Power consumption of Ion readout:

$$P_3 = P_{\text{trap}} + P_{\text{laser pulse}} + P_{\text{vacuum pump}} + P_{\text{control electronics}} + P_{\text{photon detector}}$$

-

# Power consumption of trapped-ion quantum computing

- Overall power consumption:

$$P_{\text{total}} = P_{\text{laser}} + P_{\text{supp}}$$

- $P_{\text{laser}}$ : the power consumption of laser pulse to prepare, control and readout the states.
- $P_{\text{supp}}$ : the power consumption of the supporting infrastructures, such as the ion trap, the cooling system, the vacuum pump and controlling electronics and so on.

$$P_{\text{supp}} = P_{\text{trap}} + P_{\text{vacuum}} + P_{\text{control electronics}} + P_{\text{AOM}} + \dots$$

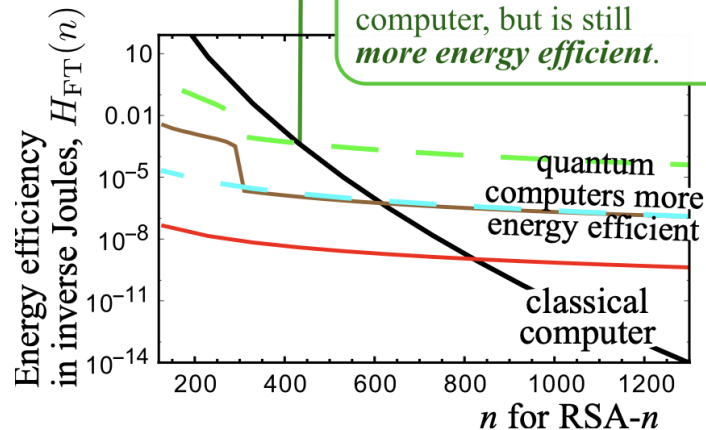
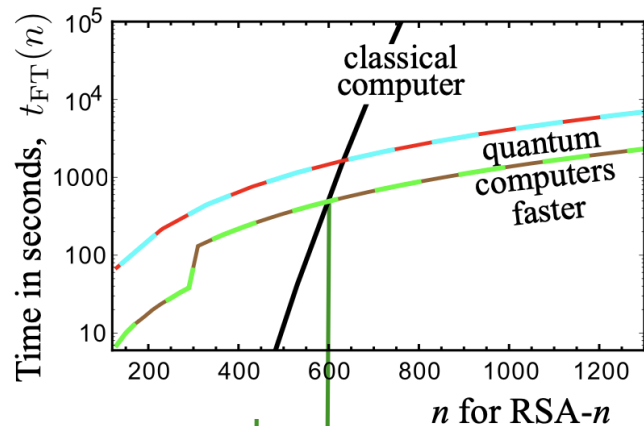
- $P_{\text{total}} \sim 1$  to 2 kW, where  $P_{\text{supp}} \gg P_{\text{laser}}$ .
- Remark:** the power consumption differs due to the different types of trapped-ion qubits, trap geometry, number of qubits, and different requirements on the quantum gates (such as the gate time).

■

# Conclusion

# Energy advantage v.s. computational advantage

- Quantum energy advantage is different from the quantum computational advantage.
- One can save energy before saving time.
- A practical advantage of different nature!



Here the green curves show a quantum computer that is *slower* than the classical computer, but is still *more energy efficient*.

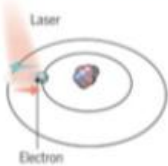
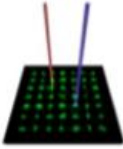
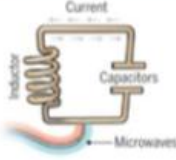

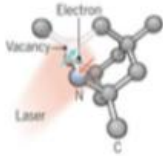
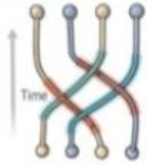
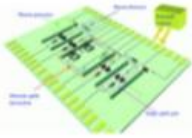
## What we already know:

- Crossover scale: Small-scale QCs pay a heavy overhead in cooling, control, and error correction. quantum energy advantage occurs for large problem size.

## Open problems:

- How to optimize the energy consumption for real quantum architectures and specific quantum algorithms?
- Which platform would be better?
- Potential for a quantum energy advantage, but
  - exist with in other problems?
  - exist for realistic quantum qubits and quantum computing architectures?

- [1] Optimising Cryogenic Wiring for Superconducting Qubit Processors in a Dilution Refrigerator A. T. Di Lonardo, J. P. Dehollain, N. K. Langford
- [2] Quantum circuits with many photons on a programmable nanophotonic chip, Xanadu Toronto Canada: <https://arxiv.org/pdf/2103.02109>
- [3] 13dB Squeezed Vacuum States at 1550nm from 12mW external pump power at 775nm  
[Axel Schönbeck, Fabian Thies, Roman Schnabel : https://arxiv.org/abs/2005.09891?](https://arxiv.org/abs/2005.09891?)
- [4] High-efficiency Thermo-optical Phase Shifter using Wave-vector and Polarization Multiplexing.  
Zhen Wang, Qihang Shang, Yong Zhang, Yikai Su : <https://otip.sjtu.edu.cn/publication/Conference/2021-ACP-ZhenWang-High-efficiency> Thermo-optical Phase Shifter using.pdf
- [5] Bernardini, Francesco, Abhijit Chakraborty, and Carlos R. Ordóñez. "Quantum computing with trapped ions: a beginner's guide." *European Journal of Physics* 45, no. 1 (2023): 013001.
- [6] Bruzewicz, Colin D., John Chiaverini, Robert McConnell, and Jeremy M. Sage. "Trapped-ion quantum computing: Progress and challenges." *Applied physics reviews* 6, no. 2 (2019).
- [7] Fellous-Asiani, Marco, Jing Hao Chai, Yvain Thonnart, Hui Khoon Ng, Robert S. Whitney, and Alexia Auffèves. "Optimizing resource efficiencies for scalable full-stack quantum computers." *PRX Quantum* 4, no. 4 (2023): 040319
- [8] Cahall, Clinton, Daniel J. Gauthier, and Jungsang Kim. "Scalable cryogenic readout circuit for a superconducting nanowire single-photon detector system." *Review of Scientific Instruments* 89, no. 6 (2018).
- [9] Cusini, Iris, Davide Berretta, Enrico Conca, Alfonso Incoronato, Francesca Madonini, Arianna Adelaide Maurina, Chiara Nonne, Simone Riccardo, and Federica Villa. "Historical perspectives, state of art and research trends of single photon avalanche diodes and their applications (part 1: Single pixels)." *Frontiers in Physics* 10 (2022): 906675.

	atoms		electron superconducting loops & controlled spin				photons
							
<b>qubit type</b>	<b>trapped ions</b>	<b>cold atoms</b>	<b>supercond.</b>	<b>silicon</b>	<b>NV centers</b>	<b>Majorana</b>	<b>photons</b>
<b>cryogeny</b>	300 W-6 kW	8-10 kW (2)	16-105 kW	12 kW	< 1 kW	16 kW	3 kW
<b>vacuum pumps<sup>1</sup></b>	ultra-vacuum	ultra-vacuum	vacuum	vacuum	vacuum	vacuum	vacuum
<b>qubits gate controls</b>	<1.4 kW ions heating, lasers, microwaves generation, CMOS readout electronics	5,8 kW atoms heater, lasers, control (SLM, AOD), readout sensor + electronics	from 20 mW to 100W / qubit depending on architectures with micro-wave generation outside or inside the cryostat		N/A	<25 mW / qubit	300 W for photons sources and detectors, qubit gates controls
<b>computing</b>	300 W	1 kW	1 kW	1 kW	<1 kW	1 kW	700 W
<b># qubits used</b>	24	100/256 (1) - 300-1000 (2)	53-433	12	<10	N/A	20
<b>total</b>	<b>2 KW (5)</b>	<b>7 (1) -20 KW (2)</b>	<b>25-140 KW (3)</b>	<b>21 KW</b>	<b>N/A</b>	<b>N/A</b>	<b>4 KW (4)</b>

<sup>1</sup> : fixed energetic cost, for preping stage

typical configurations for Pasqal and QuEra (1), neutral atoms with 4K pump/chamber cooling (2), Google Sycamore with 53 qubits, and guestimate for IBM System 2 with its KIDE cryostat(3), Quandela/QuiX (4), AQT (5) rough estimates for others

(cc) Olivier Ezratty, 2023